ce/papers Proceedings in civil engineering

Ernst & Sohn A Wiley Brand

ORIGINAL ARTICLE

eurosteel AMSTERDAM 2023

Ernst & Sohn A Wiley Brand

Memory-Steel for Smart Steel Structures: A Review on Recent Developments and Applications

Sizhe Wang[1,2] | Maryam Mohri[1] | Lingzhen Li[1,3] | Mohammadreza Izadi[4] | Ali Jafarabadi[1,3] | Niels Pichler[1,3] | Elyas Ghafoori[1,5*]

Correspondence

Prof. Dr. Elyas Ghafoori
Institute for Steel Construction
Leibniz University Hannover, Germany
Email: Ghafoori@stahl.uni-hannover.de

[1] Empa, Swiss Federal Laboratories for Materials Science and Technology, Dübendorf, Switzerland
[2] Tongji University, Shanghai, China
[3] ETH-Zürich, Zürich, Switzerland
[4] HATCH, Brisbane, Australia
[5] Leibniz University Hannover, Hannover, Germany

Abstract

This study reviews the recent works on the development and application of iron-based shape memory alloy (Fe-SMA), the so-called memory-steel, for steel structures. First, the studies on the material properties of Fe-SMA in terms of shape memory effect and superelasticity are discussed. Next, the use of Fe-SMA in prestressed strengthening of steel structures is explained, including the applications in strengthening of steel girders, connections, and fatigue crack repairs. Various strengthening solutions such as using mechanically anchored or adhesively-bonded Fe-SMA, as well as the studies on the behavior of the Fe-SMA-to-steel bonded joints, are discussed. The use and application of Fe-SMA for strengthening of a 113-years steel bridge has been explained. In addition, studies on the innovative application of the Fe-SMA as pipe couplers are presented. At the end, innovative ongoing research on the additive manufacturing of architected Fe-SMA (4D-printing) are discussed.

Keywords

memory-steel, Fe-SMA, pseudoelasticity, shape memory effect, structural strengthening, mechanical anchorage, epoxy adhesive bonding, coupler, additive manufacturing, 4D printing

1 Introduction

Shape memory alloys (SMAs) are a class of advanced materials featured for their two unique characteristics of superelasticity or pseudoelasticity (PE) and shape memory effect (SME), which are due to the presence of a reversible martensitic transformation in the crystal structure of the material [1]. The SME was first discovered by Chang and Read in 1932 in AuCd alloys; afterwards, in 1962, SME was re-discovered in a NiTi alloy by Buehler and co-researchers, and thereafter SMAs attracted a great research attention [2]. Up to date, various types of SMAs have been developed, such as NiTi-, Cu-, and Fe-based SMAs [3]. Furthermore, SMAs have gained wide applications in different fields such as mechanical engineering, aerospace industry, and medical apparatus.

In civil engineering, SMAs are also applied in many aspects, such as damping, energy dissipation, and self-centring structures, as a result of its PE behaviour, and self-actuating fasteners and couplers, concrete reinforcements, and prestressed strengthening, thanks to its SME behaviour [1-3]. The use of SMAs in civil engineering has provided innovative solutions to address different challenges such as improving the seismic performance of structures, retrofitting and strengthening existing structures, and efficient construction techniques, therefore, resulting in the improvement of the durability, resilience, and sustainability of the structures.

Among various SMAs, Fe-based SMAs (Fe-SMAs), also known as memory-steel, are highly attractive for civil engineering applications owing to their cost-effective manufacturing process and excellent mechanical properties [4]. This study reviews the recent works on the development and application of the Fe-SMA for steel structures. The topics include the development of the material, the applications of Fe-SMA in prestressed structural strengthening, experimental and theoretical developments in the use of bonded Fe-SMA, Fe-SMA couplers, and additive manufacturing of Fe-SMA.

2 Fe-SMA (memory-steel)

Fe-SMAs have excellent shape memory behaviour, mechanical properties, and cost-effectiveness, making them suitable for civil engineering applications. A novel composition of Fe-SMA, Fe–17Mn–5Si–10Cr–4Ni–1(V,C), with nano-sized VC precipitates, has been developed for civil engineering applications [5, 6]. While this alloy primarily exhibits a strong SME, making it suitable for prestressed

strengthening of civil structures, it has limited PE characteristics [7].

The limited PE of Fe-Mn-Si-based SMAs has hindered their adoption in areas such as seismic damping systems. Research has shown that PE is typically not observed in Fe-Mn-Si-based SMAs due to the nature of the martensitic transformation in these alloys. However, a combination of reversible movement of Shockley partial dislocations (SPDs) and the back transformation from ε-martensite to γ-austenite during unloading has been proposed as the microstructural explanation for PE in Fe-Mn-Si-based SMAs [8]. The PE behaviour can also be influenced by the presence of carbide precipitates and specific heat and thermomechanical treatments.

Studies by Arabi-Hashemi et al. [9] have shown that VC precipitates near the elastic strain field can significantly improve the SME and PE of the alloy. A thermomechanical treatment involving deformation at room temperature and subsequent annealing has been found to enhance the SME and PE of Fe-Mn-Si-based alloys. The treatment decreases the number of thermal twins and develops a specific texture in the austenite phase, resulting in an increased PE strain [10, 11]. Figure 1 illustrates the relationship between PE strain and $\sigma_{y0.1\%}$ (yield strength at 0.1% plastic strain) as a function of the number of thermomechanical cycles (N) for Fe-SMA sample after aging and thermomechanical treatment. The results indicated a decrease in $\sigma_{y0.1\%}$ with an increasing number of thermomechanical cycles, indicating facilitated martensite transformation and enhanced PE. It is further hypothesized that thermomechanical training increases the dislocation density and the resulting elastic strain field of the dislocations reduces the nucleation barrier for the formation of coherent martensite nuclei [10].

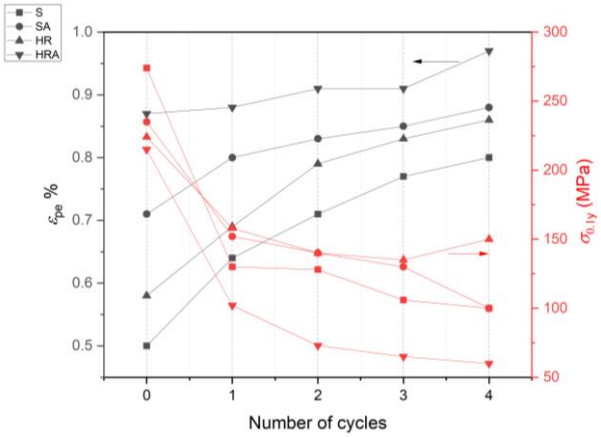

Figure 1 PE strain and 0.1% yield stress diagram versus the number of thermomechanical cycles. S: solution-annealed at 1000 °C for 2 h; SA: solution-annealed and aged at 750 °C for 6 h; HR: hot-rolled at 1000 °C; and HRA: hot-rolled and aged at 750 °C for 6 h [10].

Khodaverdi et al. [12] conducted rolling of samples at room temperature with an equivalent strain of 0.25, followed by annealing and aging processes. This resulted in a significant improvement in the alloy's performance. After applying a 4% tensile pre-straining, a residual strain of 2.85% was achieved, indicating enhanced PE (Figure 2). The absorbed energy also increased by 30%, from 17 to 22 J/cm³, demonstrating improved energy dissipation [12]. These improvements make the alloy more suitable for seismic damping applications by providing better re-centring ability after energy release. The enhancements are attributed to grain refinement, which facilitates the uniform distribution of precipitates within austenite grains during annealing and aging. Moreover, grain refinement affects the morphology and size of precipitates, leading to an increased number of stacking faults and ε-martensite volume fraction, while reducing the likelihood of ε-martensite intersection and α'-martensite formation [12].

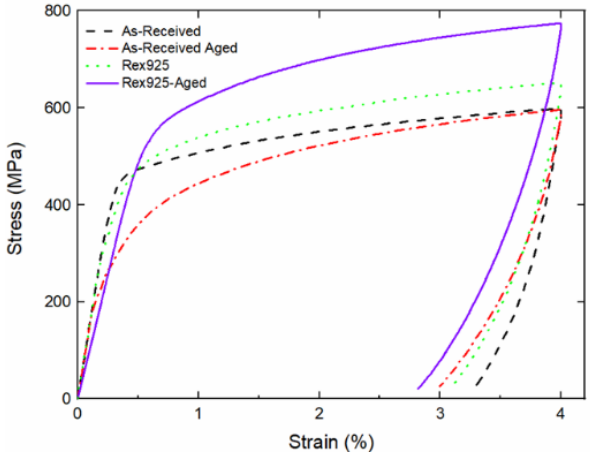

Figure 2 Loading–unloading curves of as-received, as-received aged, Rex925, and Rex925-aged samples strained to 4% in tension (Rex: recrystallization at 925 °C, ageing at 750 °C for 6h) [12].

Furthermore, studies by Khodaverdi et al. [13] indicate low-temperature aging at 485 °C in combination with high-temperature precipitates further enhances the PE of the alloy. The formation of sigma-type precipitates aligns stacking faults within the austenite grains (Figure 3), which improves the martensitic phase transformation and reduces the formation of undesired martensite phases [13].

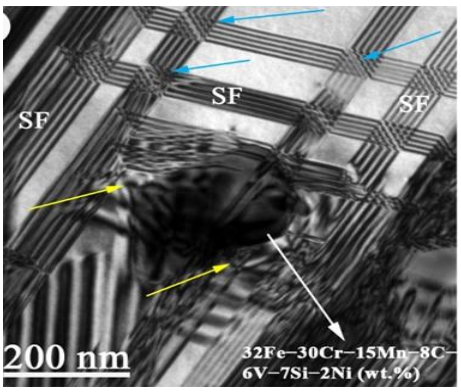

Figure 3 Bright-field TEM images of the double aged Fe-based SMA sample after a loading–unloading experiment to a peak strain of 2% in tension. Groups of parallel SFs (blue arrows) crossing each other around a precipitate in non-twinned regions of the austenite matrix, creating distorted zones around the precipitate (yellow arrows) [13].

Overall, these findings provide insights into improving the PE behaviour of Fe-SMAs, making them a promising alternative to NiTi-SMAs for seismic applications. The presence of low-temperature precipitates is beneficial in terms of manufacturing cost reduction and addressing issues related to oxidation and grain growth.

3 Strengthening of steel structures with mechanically anchored Fe-SMA

The SME of the Fe-SMA makes it a promising material for prestressed strengthening. Many studies were conducted on the application of the Fe-SMA, wherein the anchorage of the Fe-SMA to the parent structure is a key problem for the success of the application. One of the anchorage methods is mechanical anchorage. Izadi et al. [14] developed a strengthening system for steel I-beams, which involved Fe-SMA strips that were mechanically anchored by two friction-based clamps (Figure 4). The components of the anchorage systems included friction foils to enhance the friction, glass fibre reinforced polymer (GFRP) laminates o provide electrical insulation, and high-strength bolts and steel clamping plates to generate clamping forces. The SME of the Fe-SMA was activated using an electrical resistive heating method to a predefined temperature to prestress the strips. The test results indicated that Fe-SMA prestress levels of approximately 160, 330, and 430 MPa were achieved for activation temperatures of 100, 160, and 260 °C, respectively, which resulted in upward deflections of 0.7, 1.7, and 2.2 mm for the steel beam. After subjected to 2 million fatigue load cycles, no slippage in the mechanical anchorage system was observed, which indicated the reliability of the strengthening system.

Fritsch et al. [15] developed a direct-fastening technique which involved using nails to anchor Fe-SMA strips onto a steel beam. An optimized nail-anchor system which contained 12 nails (i.e., 3 × 4) was selected based on lap-shear tests and numerical analysis. A steel I-beam that was strengthened with the nail-anchored Fe-SMA strip and activated using an infrared heating technique showed an upward deflection of 0.89 mm after activation.

Izadi et al. [16, 17] studied the application of Fe-SMA strips for the fatigue strengthening of steel plates with cracks. A mechanical anchorage system consisting of clamping sets and high-strength bolts was developed to anchor the Fe-SMA strips to the steel plates. The strengthened and unstrengthened specimens were subjected to high cycle fatigue (HCF) loading. The study showed that the Fe-SMA, after an activation to 260 °C, generated a prestress level in the range of 330–410 MPa, resulting in compressive stresses of 35–72 MPa in the steel plates. The test results showed that the activated Fe-SMA strips effectively increased the fatigue life of the specimens, and in some cases, a complete fatigue crack arrest was achieved. In addition, Fe-SMA strips were used to retrofit fatigue-cracked riveted connections in steel bridges [18]. The activated Fe-SMA strips were mechanically anchored using friction-based clamps to the flanges of a steel I-beam in either side of the cracked stringer-to-floor beam double-angle connections. HCF tests were conducted and it was observed that the fatigue life was substantially enhanced by the Fe-SMA, with the fatigue crack being arrested.

Moreover, Fe-SMA was applied in strengthening a 113-year historic roadway bridge in Petrov nad Desnou, Czech Republic, which is subjected to daily passengers and heavy trucks (Figure 5) [19]. A mechanical anchorage system was developed to apply multiple Fe-SMA strips to the steel girders of the bridge. The Fe-SMA was activated using ceramic heating pads, heated to approximately 260 ◦C, and the recovery stress of the Fe-SMA strips resulted in a compressive stress of approximately −33 MPa in the lower flange of the bridge girder, which significantly increased the yield and fatigue capacity of the strengthened girder.

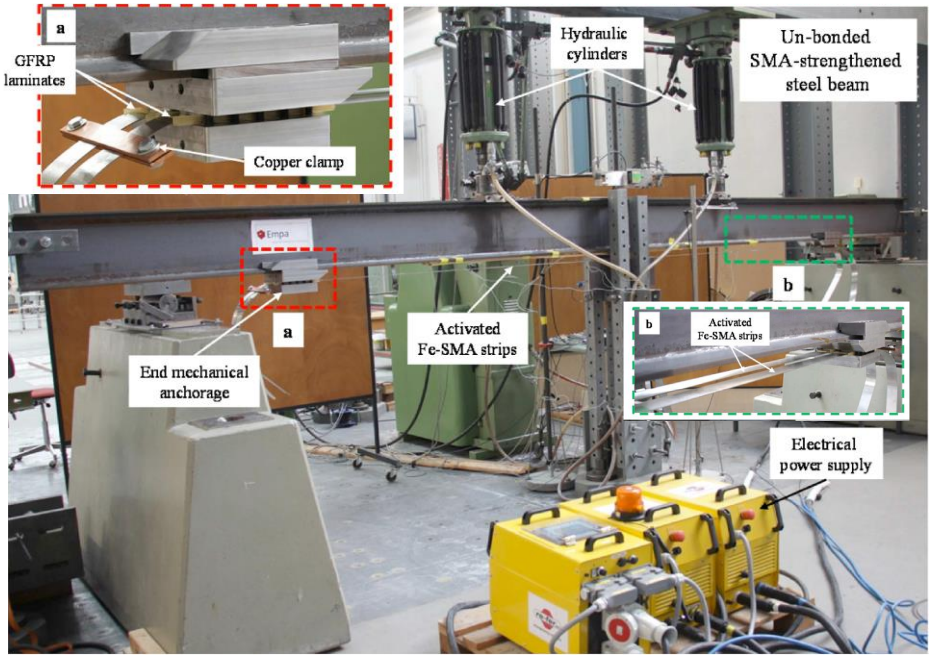

Figure 4 Experimental study on the steel beam strengthened with Fe-SMA strips anchored by friction-based clamps [14].

Figure 5 (a) A 113-years historic steel road bridge in Petrov nad Desnou, Czech Republic. (b) Configuration of the Fe-SMA-strengthened girders in Petrov Bridge [19].

4 Strengthening of steel structures with adhesively bonded Fe-SMA

The studies outlined in Section 3 have shown the potential of Fe-SMA in prestressed strengthening of steel structures. Friction-based mechanical clamps provide reliable anchorages and they can be quickly installed on site, but they are usually costly to manufacture. Nailed or bolted anchorages which involve drilling holes cause damage on the parent structures. Adhesive bonding is featured by its non-destructiveness (i.e., barely impairing the parent structures) and smooth load transfer from Fe-SMA to parent structure. Nevertheless, the capacity and durability of bonded joints are the concerns.

4.1 Strengthening solutions using bonded Fe-SMA

Aimed at developing prestressed strengthening solutions for steel beams, Wang et al. [20, 21] studied steel beams strengthened using adhesively bonded Fe-SMA strips. Two bonded solutions were proposed, i.e., partly and fully bonded solutions (Figure 6). For the partly bonded solution, the two ends of the Fe-SMA strip were adhesively bonded to the steel beam while the middle part remained unbonded. In contrast, for the fully bonded solution, the adhesive was applied along the entire surface of the Fe-SMA strip. Different activation strategies using torches were proposed for the two bonded solutions. For the partly bonded one, a two-step activation using large torch to the target temperature of 240 °C was designed (Figure 7). After activation, the Fe-SMA developed a prestress level of approximately 280 MPa, resulting in a 1 mm upward deflection of the steel beam. For the fully bonded one, the Fe-SMA was activated using a small torch to the target temperature of 140 °C. A Fe-SMA prestress of approximately 196 MPa was measured and an upward deflection of 0.73 mm was observed. A series of static and fatigue four-point bending tests under service loads were conducted, wherein no debonding or degradation was observed for the adhesively bonded Fe-SMA-strengthened specimen, which demonstrated the reliable performance of the bonded strengthening solution.

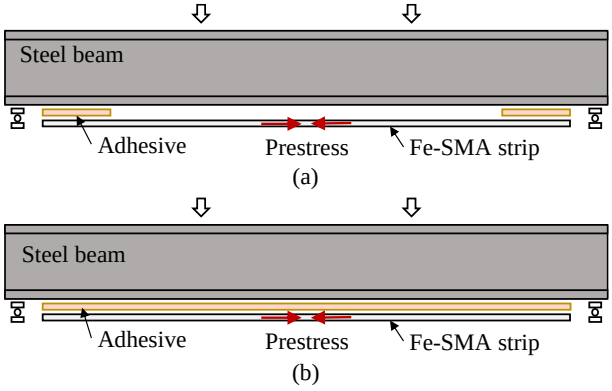

Figure 6 Strengthening solutions of steel beams using adhesively bonded Fe-SMA. (a) Partly bonded solution. (b) Fully bonded solution [20, 21].

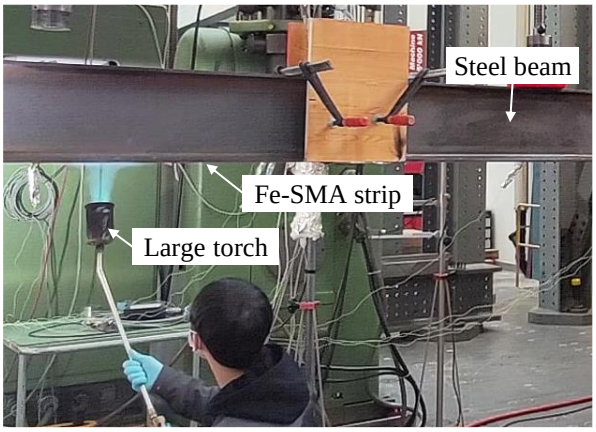

Figure 7 Activation of the Fe-SMA using a large torch in the partly bonded solution [20].

A bonded Fe-SMA solution to repair fatigue cracks of steel structures was proposed by Wang et al. [22]. Figure 8 schematically illustrates the strengthening solution. Fe-SMA strips are bonded onto the target position of the steel plate. After the adhesive is properly cured, the middle segment of the Fe-SMA strip (the activation zone) is heated to a target temperature to generate prestress, while the two ends (bonded anchorage zones), which remain unheated, transfer the generated prestress to the substrate steel plate. The solution takes advantage of the SME of Fe-SMA and the bridging mechanism offered by the bonding technique. Fatigue tests on cracked steel plates with bonded non-prestressed carbon fibre reinforced polymer (CFRP), non-prestressed Fe-SMA, and prestressed Fe-SMA

strips were conducted. The experimental results demonstrated that the bonded prestressed Fe-SMA strips extended the fatigue life of the cracked steel plates by a factor of 3.51. The repair effect of the bonded prestressed Fe-SMA was better than non-prestressed CFRP strips.

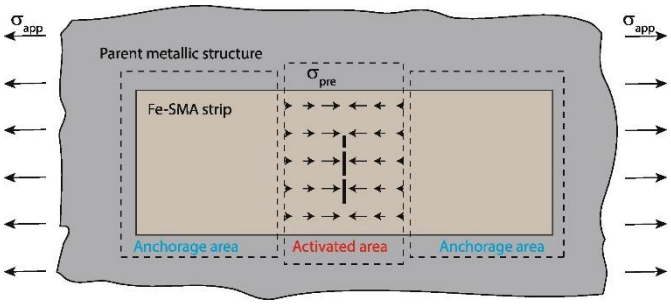

Figure 8 Schematic view of a centre-cracked steel plate strengthened by bonded prestressed Fe-SMA strips [22].

Additionally, Wang et al. [23] conducted fatigue tests on cracked steel plates strengthened by bonded Fe-SMA strips with different strip length, width, activation length, and activation strategies (i.e., heat gun, hot bonder, and gas torch). It was found that, for narrow bonded Fe-SMA strips, gas torch for activation led to the highest fatigue life extension, and when wide Fe-SMA strips were employed, fatigue crack arrests could be achieved.

Furthermore, Wang et al. [24] studied a repair solution for fatigue cracks using Fe-SMA/CFRP bonded patches. The Fe-SMA/CFRP bonded patch combines the Fe-SMA strips and CFRP sheets. The repair procedure mainly consists of three steps: bonding Fe-SMA strips, activation of Fe-SMA, and bonding CFRP sheets. The design concept is that the activated Fe-SMA strip can offer both stiffness and prestress, while the CFRP sheet can provide additional stiffness and protection for the prestressed Fe-SMA against corrosions. Fatigue tests were conducted and the typical failure modes of the repaired specimens were as shown in Figure 9. Fatigue test results indicated that both the bonded Fe-SMA and the bonded Fe-SMA/CFRP patch could substantially extend the fatigue life, with an extension ration of ≥4.2 and ≥5.5, respectively. Moreover, the experimental study demonstrated that a small-sized repair patch with the Fe-SMA strip length as short as 100 mm was feasible and effective.

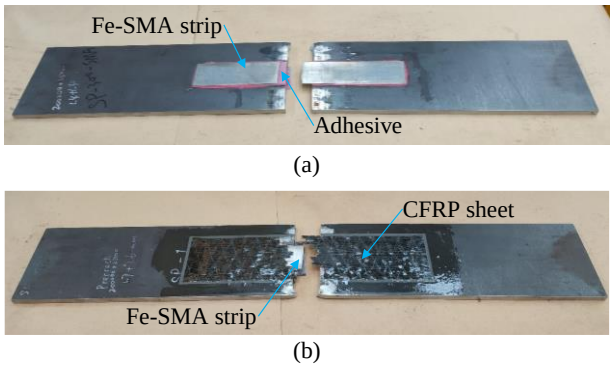

Figure 9 (a) Typical failure mode of bonded Fe-SMA-strengthened steel plate. (b) Typical failure mode of bonded Fe-SMA/CFRP patch-strengthened steel plate [24].

Li et al. [25] proposed two models for the analysis of strain and deformation of bonded Fe-SMA strengthened steel structures, validated by experiments from the literature. A design recommendation, in line with Eurocode 0 [26], was proposed with an outlook involving possible future investigations. Based on the proposed prestress analysis models [25], Li et al. [27] further proposed an analytical model, comprising a prestress analysis and a fatigue crack analysis, for modelling the behaviour of central-cracked steel plates strengthened by bonded Fe-SMA strips. Four central-cracked steel plates were strengthened by bonded Fe-SMA strips and tested under fatigue loading regimes. The fatigue crack arrest was achieved experimentally after activation of prestress. The test results showed that the proposed analytical model is capable of predicting the onset of fatigue crack propagation after strengthening.

4.2 Fe-SMA-to-steel bonded joints

The successful application of the bonded Fe-SMA strengthening solutions highly relies on the bonded joint, so a robust understanding of the bond behaviour between Fe-SMA strips and steel substrates should be established. The research group conducted intensive investigations to characterize the Fe-SMA-to-steel adhesively bonded joints.

In order to acquire a reliable and durable bonding performance, Pichler et al. [28] investigated the influence of several surface preparation techniques (UV/ozone exposure, sol-gel, and primers) on the adhesion and durability of Fe-SMA bonded joints with different adhesives. The floating-roller peel tests was used to assess the joint failure mode, and exposure in a salt-spray cabinet was used to discriminate which joint was the most durable. The application of sol-gel was identified as a crucial step to achieve a complete cohesion failure. SikaPower-1277 adhesive in combination with sol-gel and primer exhibited minimal corrosion effect.

Adhesively bonded joints are typically subjected to two modes of loading, i.e., opening mode (mode-I) and shear mode (mode-II), or a combination of both modes (mixed-modes). Due to the early onset of material nonlinear behaviour induced by the phase transformation of the Fe-SMA, conventional joint failure analysis methods are usually not applicable.

Pichler [29] proposed a fast and accurate numerical solution to the mode-I debonding process employing double cantilever beam samples (Figure 10a), which is consistent with finite element simulation and validated experimentally. This numerical solution is capable of analysing bonded joints with linear and nonlinear adherents which are bonded by adhesives with arbitrary traction-separation behaviours and showed that the onset of phase transformation prior to joint failure greatly reduced the joint strength.

In order to understand the mode-II debonding behaviour, incorporating the nonlinearity of both adherents and adhesives, Wang et al. [30] and Li et al. [31-33] performed experiments, analytical modelling, and numerical modelling of Fe-SMA-to-steel lap-shear joints (Figure 10b). Wang et al. [30] and Li et al. [31] conducted a series of lap-shear tests to investigate the effect of different Fe-SMA strips (non-prestrained and prestrained), adhesives (linear and nonlinear), and adhesive thicknesses. The test

results were compared against CFRP-to-steel lap-shear joints comprising identical adhesive and similar geometry. It was found that among Fe-SMA bonded joints, non-linear adhesives provide much higher bond capacities than linear adhesives; when linear adhesives are used in bonding, Fe-SMA joints behave similarly to CFRP joints, whereas when nonlinear adhesives are used in bonding, a clear difference between Fe-SMA and CFRP bonded joints is resulting from the difference between the nonlinear Fe-SMA behaviour and linear elastic CFRP behaviour.

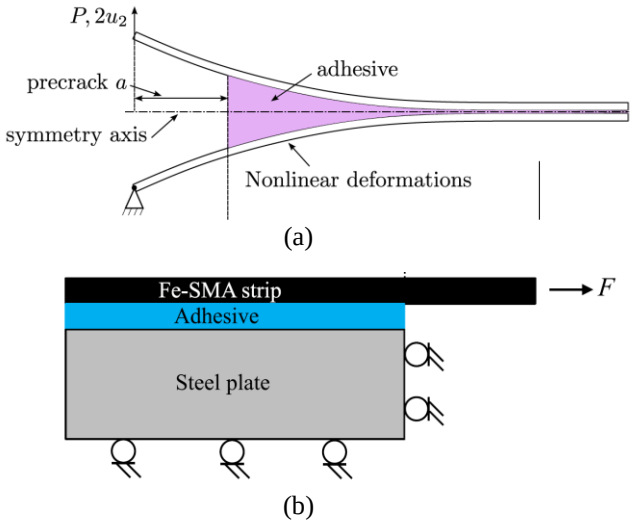

Figure 10 (a) Double cantilever beam model [29], and (b) lap-shear model [31] for the investigation of the mode-I and –II debonding behaviour, respectively.

To replicate the experimental results and facilitate future design, Li et al. [32] proposed an analytical model for the prediction of bond capacity and inference of the bond-slip behaviour. A numerical scheme was further proposed to analyse the full-range behaviour. These analytical and numerical models were validated on experimental measurements. Since the bond-slip behaviour plays a crucial role in the analysis and modelling of the debonding behaviour, Li et al. [33] performed in-depth numerical analysis of Fe-SMA lap-shear joints comprising different adhesive types with different bond-slip behaviours. The modelled full-range behaviour was scrutinized and compared with the experimental measurements. The results determined that the bond-slip behaviour of linear and nonlinear adhesives possess a triangular and a trapezoidal pattern, respectively.

The above investigations were conducted at room temperature, targeting at investigating the bonded anchorage zone. In order to investigate the effect of activation temperature and generated prestress on the bond behaviour (the activation zone), Li et al. [34] conducted lap-shear tests and analysis on Fe-SMA-to-steel lap-shear joints with activation. The tests and a thermal analysis confirmed that the bonded anchorage zone is an indispensable component to the strengthening system, without which the entire bond fails during the activation process. The analysis of the full-range behaviour suggests that the load-displacement behaviour and bond-slip behaviour prior to and after activation are interchangeable. This reveals the potential in employing the bond-slip behaviour of non-activated joints in the design of bonded Fe-SMA strengthening.

5 Memory-steel pipe couplers

Memory-steel pipe couplers (MSPCs) have been widely investigated through numerous studies. Several advantages such as quick assembly process and possibility of utilization in limited work spaces together with the reasonable price have positioned MSPCs as an appealing alternative for traditional welded and bolted joints. Application of MSPCs requires two working steps, including the pre-straining and activation (Figure 11a). Initially, MSPC is manufactured with a smaller inner diameter than the outer diameter of target pipe. Then, through pre-straining process the inner diameter will be expanded to a diameter larger than the outer diameter of the pipe in order to provide enough clearance for MSPC to be inserted at the pipe joint. After MSPC is installed, activation can be conducted through heating the joint to trigger the SME. Early feasibility studies have shown no leakage under hydrostatic tests up to 40 MPa [35]. MSPCs were successfully employed in Wakunami tunnel in Japan, soon after the preliminary studies (Figure 11b) [36-38]. Li et al. [39] reported 20 kN tensile strength while maintaining a sealing threshold of 5 MPa for MSPC of dimeter 30 mm, which satisfy the requirements for pipe jointing in general industrial applications. Druker et al. [40] have reported on the formability and weldability of Fe-SMA sheets processed for manufacturing of MSPCs. In order to examine the performance of the joints under dynamic loads, Cao et al. [41-43] conducted a comprehensive series of studies where axial and bending strength of MSPCs were characterized for low and high velocity impact loads. The results indicated a great potential for utilizing MSPCs on an industrial scale as pipeline coupling solutions. Given the importance of development of hydrogen pipeline network infrastructure as pillar of energy transition in Europe, MSPCs are appealing solutions to facilitate this transition.

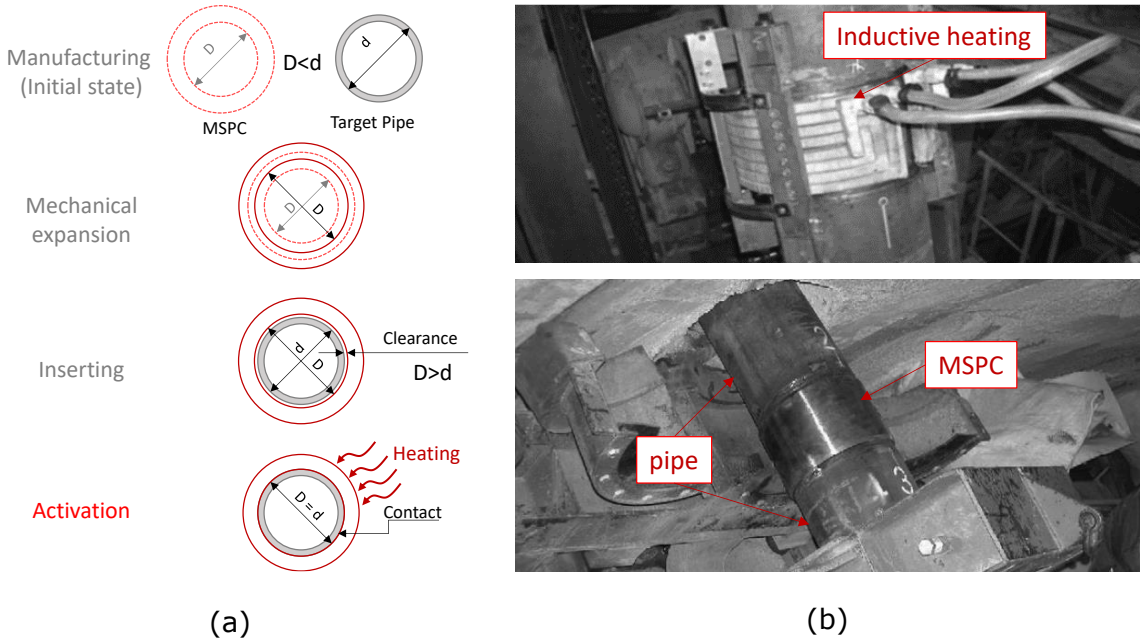

Figure 11 (a) Working mechanism of MSPCs. (b) Photographs of the MSPCs employed in the construction of the Wakunami Tunnel in Kanazawa, Japan [36, 37].

6 Additive Manufacturing of Fe-SMA

The application of SMAs in additive manufacturing (AM) technology provides a unique capability that the AMed parts can recover the original shape after being deformed, so-called 4D printing process [46] and [47]. However, AM processes can introduce defects, such as porosity, in the final components, which may affect the structural integrity of metals [48] and [49]. Fe-based SMAs can be sensitive to defects, which may adversely affect their shape memory and mechanical properties. Optimizing parameters should consider minimizing defects in the final printed parts. AM can lead to microstructural variability within the printed parts. This variability can impact the material's properties and response, making it challenging to predict the performance accurately. Optimizing parameters to regulate the functionality of additive manufactured Fe-based SMA indeed has its challenges and potential drawbacks. Fe-based SMAs are complex materials with intricate phase transformation behavior, which can make the optimization process difficult. Accurate characterization of the material properties, including transformation temperatures, phase stability, and mechanical behavior, is crucial for successful parameter optimization; however, the understanding of the underlying mechanisms governing the behavior of Fe-based SMAs is still evolving.

Recently, some studies have been done on Fe-SMAs and results indicated that a complex 3D geometry of Fe-SMAs can be produced by laser powder bed fusion (L-PBF) [44]. In addition, AMed samples display a higher SME compared to conventionally manufactured alloys with the same composition [45]. Moreover, the influence of thermomechanical treatment on SME and PE of AMed Fe-SMA was studied, and results show that although thermomechanical training led to improved PE, it reduced the SME (Figure 12) [11].

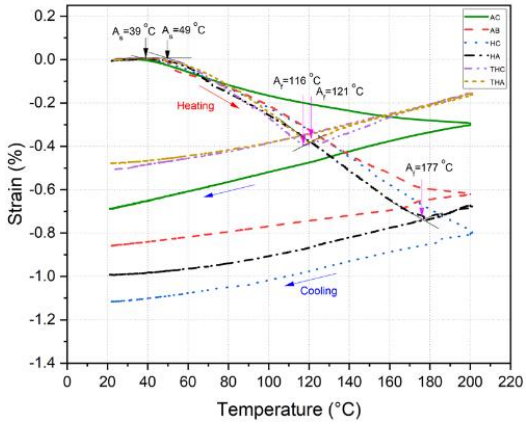

Figure 12 Recovery strain as a function of temperature after 4% strain for conventional and additive manufactured samples; AC: As-received conventional, AB: As-built additive manufactured, HC: Heat-treated conventional, THC: Trained heat-treated conventional, HA: Heat-treated additive manufactured, THA: Trained heat treated additive manufactured samples [11].

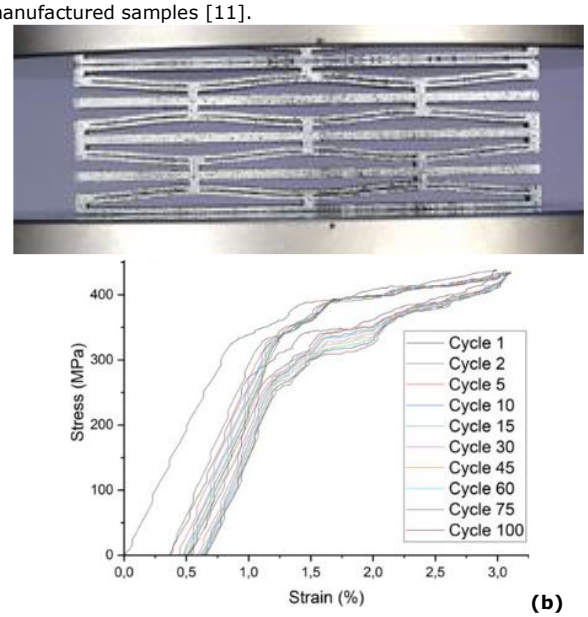

Figure 13 (a) 4D-printed architected steel structure [47]. (b) Cycling behaviour of Fe-SMA specimen [46].

Fe-SMA walls have recently been fabricated using wire arc additive manufacturing (WAAM) (Figure 13). The WAAM-fabricated Fe-SMAs exhibited negligible porosity and high deposition efficiency. Microstructural characterization revealed that the as-built samples are primarily composed by austenitic phase. Tensile and cyclic testing highlighted the excellent mechanical and functional response of the Fe-SMAs. The cyclic stability during 100 load/unloading cycles was also evaluated (Figure 13b), showcasing the potential applicability of the fabricated material for structural applications [46]. In addition, Fe-SMA lattice structures in the shape of honeycombs were manufactured using L-PBF [47]. The extraordinary results demonstrated the multi-functionality of 4D printed cellular structure by combining the smart material and manufacturing technique.

7 Conclusions

Owing to the properties of SME and PE, SMAs show promising potentials for smart and sustainable solutions for civil engineering and in particular steel construction. This study provides an overview of the recent works on the development and applications of memory-steel (i.e., Fe-SMA) for steel structures. Development of materials with high performance and cost-effective production process is an important focus in the SMA-related filed. The applications of Fe-SMA in strengthening of steel girders, enhancing connections, repairing fatigue cracks, and use as couplers are discussed. To this end, knowledge on the behaviour of the SMA-based structures, such as the static and fatigue behaviours of the mechanically anchored or adhesively bonded Fe-SMA, is necessary for engineering design. Furthermore, additive manufacturing of Fe-SMA, the so-called 4D printing, which shows great potential for realization of complex geometries, is discussed. Although the research and application of Fe-SMA have gained significant progress in recent years, there is still intensive need for continued research in this field to promote the further development for construction sector.

References

[1] L. Janke, C. Czaderski, M. Motavalli, J. Ruth, Applications of shape memory alloys in civil engineering structures—Overview, limits and new ideas, Materials and Structures 38(5) (2005) 578-592.

[2] G. Song, N. Ma, H.N. Li, Applications of shape memory alloys in civil structures, Eng. Struct. 28(9) (2006) 1266-1274.

[3] E. Ghafoori, B. Wang, B. Andrawes, Shape memory alloys for structural engineering: An editorial overview of research and future potentials, Eng. Struct. 273 (2022) 115138.

[4] A. Cladera, B. Weber, C. Leinenbach, C. Czaderski, M. Shahverdi, M. Motavalli, Iron-based shape memory alloys for civil engineering structures: An overview, Constr. Build. Mater. 63 (2014) 281-293.

[5] C. Leinenbach, H. Kramer, C. Bernhard, D. Eifler, Thermo-Mechanical Properties of an Fe–Mn–Si–Cr–Ni–VC Shape Memory Alloy with Low Transformation Temperature, Advanced Engineering Materials 14(1-2) (2012) 62-67.

[6] Z. Dong, U.E. Klotz, C. Leinenbach, A. Bergamini, C. Czaderski, M. Motavalli, A Novel Fe-Mn-Si Shape Memory Alloy With Improved Shape Recovery Properties by VC Precipitation, Advanced Engineering Materials 11(1-2) (2009) 40-44.

[7] X.-L. Gu, Z.-Y. Chen, Q.-Q. Yu, E. Ghafoori, Stress recovery behavior of an Fe-Mn-Si shape memory alloy, Eng. Struct. 243 (2021) 112710.

[8] A. Sato, E. Chishima, K. Soma, T. Mori, Shape memory effect in γ⇄ε transformation in Fe-30Mn-1Si alloy single crystals, Acta Metallurgica 30(6) (1982) 1177-1183.

[9] A. Arabi-Hashemi, W.J. Lee, C. Leinenbach, Recovery stress formation in FeMnSi based shape memory alloys: Impact of precipitates, texture and grain size, Materials & Design 139 (2018) 258-268.

[10] M. Mohri, I. Ferretto, C. Leinenbach, D. Kim, D.G. Lignos, E. Ghafoori, Effect of thermomechanical treatment and microstructure on pseudo-elastic behavior of Fe–Mn–Si–Cr–Ni-(V, C) shape memory alloy, Materials Science and Engineering: A 855 (2022) 143917.

[11] M. Mohri, I. Ferretto, H. Khodaverdi, C. Leinenbach, E. Ghafoori, Influence of thermomechanical treatment on the shape memory effect and pseudoelasticity behavior of conventional and additive manufactured Fe–Mn–Si–Cr–Ni-(V,C) shape memory alloys, Journal of Materials Research and Technology 24 (2023) 5922-5933.

[12] H. Khodaverdi, M. Mohri, E. Ghafoori, A.S. Ghorabaei, M. Nili-Ahmadabadi, Enhanced pseudoelasticity of an Fe–Mn–Si-based shape memory alloy by applying microstructural engineering through recrystallization and precipitation, Journal of Materials Research and Technology 21 (2022) 2999-3013.

[13] H. Khodaverdi, M. Mohri, A.S. Ghorabaei, E. Ghafoori, M. Nili-Ahmadabadi, Effect of low-temperature precipitates on microstructure and pseudoelasticity of an Fe–Mn–Si-based shape memory alloy, Materials Characterization 195 (2023) 112486.

[14] M. Izadi, A. Hosseini, J. Michels, M. Motavalli, E. Ghafoori, Thermally activated iron-based shape memory alloy for strengthening metallic girders, Thin-Walled Struct. 141 (2019) 389-401.

[15] E. Fritsch, M. Izadi, E. Ghafoori, Development of nail-anchor strengthening system with iron-based shape memory alloy (Fe-SMA) strips, Constr. Build. Mater. 229 (2019) 14.

[16] M.R. Izadi, E. Ghafoori, M. Motavalli, S. Maalek, Iron-based shape memory alloy for the fatigue strengthening of cracked steel plates: Effects of re-activations and loading frequencies, Eng. Struct. 176 (2018) 953-967.

[17] M.R. Izadi, E. Ghafoori, M. Shahverdi, M. Motavalli, S. Maalek, Development-of an iron-based shape memory alloy (Fe-SMA) strengthening system for steel plates, Eng. Struct. 174 (2018) 433-446.

[18] M. Izadi, M. Motavalli, E. Ghafoori, Iron-based shape memory alloy (Fe-SMA) for fatigue strengthening of cracked steel bridge connections, Constr. Build. Mater. 227 (2019) 17.

[19] J. Vůjtěch, P. Ryjáček, J. Campos Matos, E. Ghafoori, Iron-Based shape memory alloy for strengthening of 113-Year bridge, Eng. Struct. 248 (2021) 113231.

[20] S. Wang, L. Li, Q. Su, X. Jiang, E. Ghafoori, Strengthening of steel beams with adhesively bonded memory-steel strips, Thin-Walled Struct. 189 (2023) 110901.

[21] S. Wang, L. Li, Q. Su, X. Jiang, E. Ghafoori, Experimental study on steel girder strengthened with adhesively bonded iron-based shape memory alloy, The Sixth International Conference on Smart Monitoring, Assessment and Rehabilitation of Civil Structures (SMAR 2022), Shanghai, China, 2022.

[22] W. Wang, L. Li, A. Hosseini, E. Ghafoori, Novel fatigue strengthening solution for metallic structures using adhesively bonded Fe-SMA strips: A proof of concept study, Int. J. Fatigue 148 (2021) 106237.

[23] W. Wang, Y.e. Ma, E. Ghafoori, M. Motavalli, Complete fatigue crack arrest using bonded prestressed Fe-SMA repairs, International Journal of Fatigue (under review).

[24] S. Wang, Q. Su, X. Jiang, M. Motavalli, E. Ghafoori, Development of repair solution for fatigue cracks using self-prestressing Fe-SMA/CFRP bonded patches, 11th International Conference on Fiber-Reinforced Polymer (FRP) Composites in Civil Engineering (CICE 2023), Rio de Janeiro, Brazil, 2023.

[25] L. Li, S. Wang, E. Chatzi, M. Motavalli, E. Ghafoori, Analysis and Design Recommendations for Structures Strengthened by Prestressed Externally Bonded Fe-SMA Strips, Materials & Design (under review).

[26] European Committee for Standardization. BS EN 1990:2002. Eurocode — Basis of structural design, 2002.

[27] L. Li, S. Wang, T. Chen, E. Chatzi, H. Heydarinouri, E. Ghafoori, Fatigue strengthening of cracked steel plates with bonded Fe-SMA strips, 10th EuroSteel conference, Amsterdam, Neatherland, 2023.

[28] N. Pichler, W. Wang, J.A. Poulis, E. Ghafoori, Surface preparations and durability of iron-based shape memory alloy adhesively-bonded joints, International Journal of Adhesion and Adhesives (2023) 103439.

[29] N. Pichler, Mode I Fracture Analysis of Fe-SMA Bonded Joints as Nonlinear Elastic Beam on Foundation (A chapter of PhD thesis), ETH-Zurich, Zurich, Switerland, to be submitted in 2024.

[30] W. Wang, A. Hosseini, E. Ghafoori, Experimental study on Fe-SMA-to-steel adhesively bonded interfaces using DIC, Engineering Fracture Mechanics 244 (2021) 107553.

[31] L. Li, W. Wang, E. Chatzi, E. Ghafoori, Experimental investigation on debonding behavior of Fe-SMA-to-steel joints, Constr. Build. Mater. 364 (2023) 129857.

[32] L. Li, E. Chatzi, E. Ghafoori, Debonding model for nonlinear Fe-SMA strips bonded with nonlinear adhesives, Engineering Fracture Mechanics 282 (2023) 109201.

[33] L. Li, E. Martinelli, W. Wang, E. Chatzi, E. Ghafoori, Bond-Slip Behavior of Nonlinear Fe-SMA Lap-Shear Joints, Structures (under review).

[34] L. Li, E. Chatzi, C. Czaderski, E. Ghafoori, Influence of Activation Temperature and Prestress on Be-havior of Fe-SMA Bonded Joints, Construction and Building Materials (under review).

[35] D.Z. Liu, W.X. Liu, F.Y. Gong, Engineering Application of Fe-Based Shape Memory Alloy on Connecting Pipe Line, J. Phys. IV France 05(C8) (1995) C8-1241-C8-1246.

[36] H. Otsuka, H. Tanahashi, T. Maruyama, M. Murakami, H. Yamada, Development of Fe-Mn-Si shape memory alloys for pipe joints in steel construction, Materia Japan 37(4) (1998) 283-285.

[37] T. Maruyama, H. Kubo, 12 - Ferrous (Fe-based) shape memory alloys (SMAs): properties, processing and applications, in: K. Yamauchi, I. Ohkata, K. Tsuchiya, S. Miyazaki (Eds.), Shape Memory and Superelastic Alloys, Woodhead Publishing2011, pp. 141-159.

[38] T. Sawaguchi, T. Maruyama, H. Otsuka, A. Kushibe, Y. Inoue, K. Tsuzaki, Design Concept and Applications of Fe–Mn–Si-Based Alloys—from Shape-Memory to Seismic Response Control, MATERIALS TRANSACTIONS 57(3) (2016) 283-293.

[39] J.C. Li, M. Zhao, Q. Jiang, Comparison of shape memory effect between casting and forged alloys of Fe14Mn6Si9Cr5Ni, Journal of Materials Engineering and Performance 11(3) (2002) 313-316.

[40] A.V. Druker, A. Perotti, I. Esquivel, J. Malarría, A manufacturing process for shaft and pipe couplings of Fe–Mn–Si–Ni–Cr shape memory alloys, Materials & Design (1980-2015) 56 (2014) 878-888.

[41] B. Cao, T. Iwamoto, A strength prediction of joints by Fe-Mn-Si-Cr shape memory alloy through strain monitoring during pre-processes including diameter expansion and tightening by heating, Engineering Fracture Mechanics 284 (2023) 109234.

[42] B. Cao, Q. Sun, T. Iwamoto, Bending fracture strength of the pipe joint using iron-based shape memory alloy (Fe-SMA) subjected to different expansion methods at various deformation rates, Eng. Struct. 267 (2022) 114669.

[43] B. Cao, Q. Sun, T. Iwamoto, Effect of deformation rate on the axial joint strength made of Fe-SMA, Journal of Constructional Steel Research 191 (2022) 107193.

[44] I. Ferretto, D. Kim, N.M. Della Ventura, M. Shahverdi, W. Lee, C. Leinenbach, Laser powder bed fusion of a Fe–Mn–Si shape memory alloy, Additive Manufacturing 46 (2021) 102071.

[45] I. Ferretto, D. Kim, M. Mohri, E. Ghafoori, W.J. Lee, C. Leinenbach, Shape recovery performance of a (V, C)-containing Fe–Mn–Si–Ni–Cr shape memory alloy fabricated by laser powder bed fusion, Journal of Materials Research and Technology 20 (2022) 3969-

3984.

[46] I.O. Felice, J. Shen, A.F.C. Barragan, I.A.B. Moura, B. Li, B. Wang, H. Khodaverdi, M. Mohri, N. Schell, E. Ghafoori, T.G. Santos, J.P. Oliveira, Wire and arc additive manufacturing of Fe-based shape memory alloys: Microstructure, mechanical and functional behavior, Materials & Design 231 (2023) 112004.

[47] A. Jafarabadi, I. Ferretto, M. Mohri, C. Leinenbach, E. Ghafoori, 4D Printing of Recoverable Buckling-Induced Architected Iron-based Shape Memory Alloys, Materials and Design, 2023 (accepted).

[48] C Huang, Y Zheng, T Chen, E Ghafoori, L Gardner, Fatigue crack growth behaviour of wire arc additively manufactured steels, International Journal of Fatigue 173 (2023), 107705

[49] C Huang, L Li, N Pichler, E Ghafoori, L Susmel, L Gardner, Fatigue testing and analysis of steel plates manufactured by wire-arc directed energy deposition, Additive Manufacturing, 103696 (2023).